TISSUE ENGINEERING: Part A
Volume 19, Numbers 7 and 8, 2013

DOI: 10.1089/ten.tea.2012.0111

Novel Polypyrrole-Coated Polylactide Scaffolds Enhance Adipose Stem Cell Proliferation and Early Osteogenic Differentiation

Jani Pelto, MSc,[1] Miina Björninen, MSc,[2–4] Aliisa Pälli, MSc,[2–4] Elina Talvitie, MSc,[4,5] Jari Hyttinen, PhD,[4,5] Bettina Mannerström, PhD,[2–4] Riitta Suuronen Seppanen, MD, DDS,[2,4–6] Minna Kellomäki, PhD,[4,5] Susanna Miettinen, PhD,[2–4] and Suvi Haimi, PhD[2–4,7]

An electrically conductive polypyrrole (PPy) doped with a bioactive agent is an emerging functional biomaterial for tissue engineering. We therefore used chondroitin sulfate (CS)-doped PPy coating to modify initially electrically insulating polylactide resulting in novel osteogenic scaffolds. *In situ* chemical oxidative polymerization was used to obtain electrically conductive PPy coating on poly-96L/4D-lactide (PLA) nonwoven scaffolds. The coated scaffolds were characterized and their electrical conductivity was evaluated in hydrolysis. The ability of the coated and conductive scaffolds to enhance proliferation and osteogenic differentiation of human adipose stem cells (hASCs) under electrical stimulation (ES) in three-dimensional (3D) geometry was compared to the noncoated PLA scaffolds. Electrical conductivity of PPy-coated PLA scaffolds (PLA-PPy) was evident at the beginning of hydrolysis, but decreased during the first week of incubation due to de-doping. PLA-PPy scaffolds enhanced hASC proliferation significantly compared to the plain PLA scaffolds at 7 and 14 days. Furthermore, the alkaline phosphatase (ALP) activity of the hASCs was generally higher in PLA-PPy seeded scaffolds, but due to patient variation, no statistical significance could be determined. ES did not have a significant effect on hASCs. This study highlights the potential of novel PPy-coated PLA scaffolds in bone tissue engineering.

Introduction

Polylactide-based polymers have been extensively used in various applications for over two decades. However, lack of bioactivity has limited their use especially in tissue engineering applications.[1,2] To overcome this problem, several approaches have been developed, such as integrating growth factors, or other bioactive agents into the polymer structure.[3,4] Another potential strategy to functionalize polylactide scaffolds could be the application of conductive polymers as a functional surface coating. Among these conductive polymers, polypyrrole (PPy) has emerged as a promising polymer group for tissue engineering due to its high biocompatibility and its good electroconductive properties.[5]

The surface roughness, hydrophilicity, and elasticity of PPys can be tailored by the choice of the dopants or surfactants used in their synthesis.[6,7] One of the most studied biopolymer dopants is chondroitin sulfate (CS), a naturally occurring ubiquitous glycosaminoglycan.[8,9] CS is found not only in the ECM, but was also discovered on the cell surfaces of most mammalian cells and reported to be involved in osteogenic processes, including development, maturation, remodeling, and repair.[10,11] CS has previously been shown to enhance bone remodeling when applied together with hydroxyapatite/collagen bone cement.[9] Due to the osteogenic potential of CS, we hypothesized that by using CS-doped PPy coating, we could stimulate the osteogenic differentiation of human adipose stem cells (hASCs), a potential mesenchymal stem cell (MSC) group in the field of skeletal tissue engineering.

In an earlier study, we already verified the good biocompatibility of PPy using hASCs.[7] The effect of PPy surfaces with or without electrical stimulation (ES) has been studied with various cell types, such as skeletal muscle cells, neurites, endothelial cells, fibroblasts, osteoblasts, and

[1]VTT Technical Research Centre of Finland, Tampere, Finland.
[2]Adult Stem Cells, Institute of Biomedical Technology, University of Tampere, Tampere, Finland.
[3]Science Centre, Pirkanmaa Hospital District, Tampere, Finland.
[4]BioMediTech, Tampere, Finland.
[5]Department of Biomedical Engineering, Tampere University of Technology, Tampere, Finland.
[6]Department of Eye, Ear, and Oral Diseases, Tampere University Hospital, Tampere, Finland.
[7]Department of Biomaterials Science and Technology, University of Twente, Enschede, Netherlands.

MSCs.[12–17] However, so far, the effects of PPy on osteogenic differentiation of human ASCs have not, to the best of our knowledge, been reported either with or without ES.

ES has been applied to a number of cell types to enhance proliferation and to direct cell differentiation, but mainly to electrically active cells, such as neurons or cardiomyoblasts.[18] Interestingly, a few recent publications have focused on the stimulation of electrically inactive MSCs, demonstrating that ES has a significant impact on ASC proliferation and differentiation.[19–21] ES has also been successfully applied via PPy for different cell types resulting in increased cell proliferation and significant changes in other cell functions.[22–24] This article is the first to report the effects of novel conductive poly-96L/4D-lactide/PPy (PLA-PPy) scaffolds and their combined effects with the ES on hASC viability, proliferation, and early osteogenic differentiation studied in a three-dimensional (3D) culture system.

Materials and Methods

Materials

Medical grade PLA with an inherent viscosity of 2.1 dL g-1 (PURAC biochembv) was used in melt spinning and scaffold manufacturing. Pyrrole monomer, ammonium peroxydisulfate oxidant (APS), and chondroitin 6-sulfate sodium salt from bovine trachea were purchased from Sigma-Aldrich. Pyrrole was distilled in a vacuum before use. Other reagents were used without any further purification. Distilled water was used in the polymerizations.

Synthesis of 3D scaffolds

Polylactide fibers and nonwoven scaffolds. PLA was extruded (GimacMicroextruder TR 12/24 B.V.O.; Gimac) and hot-drawn to 16ply multifilament fiber. The diameters of the single filaments were 10–20 μm. To manufacture the nonwoven scaffolds, the fibers were cut and carded using a manually operated drum carder (Elite Drum Carder; Louët BV). Several cards were then combined by needle punching using a James Hunter Needle Punching Machine (James Hunter Machine Co.) to obtain $10 \times 10 \times 2$ mm size scaffolds.

Chemical oxidative polymerization of PPy. The polymerization parameters were optimized to ensure optimal conductivity and uniformity of the coating; the pyrrole concentration varied between 0.03–0.3 M, the CS concentration between 0.5–2 mg/mL, the oxidant concentration between 0.01–0.1M, and the polymerization time from 30 s to 15 min in an ambient temperature. The following optimized concentrations were used for all the *in vitro* samples: [pyrrole] = 0.036 M, [APS] = 0.1 M, and [CS] = 1 mg/mL, polymerization time 150 s.

Before polymerization, CS and APS were dissolved separately in distilled water. CS and APS solutions were combined and pyrrole added immediately with vigorous stirring. The sample was placed in the polymerization bath. The nonwoven scaffolds were pretreated in ethanol before polymerization. After polymerization, the samples were rinsed thoroughly with water and dried in air. Samples were sterilized by gamma irradiation (BBF Sterilizations service GmbH) with an irradiation dose of >25 kGy.

Characterization

Hydrolysis and conductivity measurements. Gamma irradiated scaffolds were incubated in sealed plastic specimen chambers containing either a phosphate buffer solution PBS (Sörensen, pH 7.4 ± 0.2; Na_2HPO_4 0.0546 mol l-1, KH_2PO_4 0.121 mol l-1) or a maintenance medium consisting of the Dulbecco's modified Eagle's medium/Ham's Nutrient Mixture F-12 (DMEM/F-12 1:1 1 ×; Invitrogen), 10% human serum type AB (HS; PAA Laboratories GmbH), 1% L-glutamine (GlutaMAX I; Invitrogen), and 1% pen-strep (100 U/mL penicillin, 0.1 mg/mL streptomycin; Lonza) at +37°C for up to 42 days. Test conditions were set as specified in ISO-15814:1999(E) standard. The pH of the buffer solution was measured and changed every 3 days twice a week to exclude the acidic autocatalytic hydrolysis of PLA.

Directly after the synthesis and during the hydrolysis test, the direct current (DC) conductivity of air-dry scaffolds was measured using custom-made copper flat alligator clips (contact area 6 mm^2) and Fluke 189 multimeter. Non-sterilized samples were used for conductivity measurement since the electrical properties of PPy have been reported to be stable[25] with the irradiation dose used.

Electrospray ionization mass spectroscopy. Gamma-sterilized, noncoated PLA and PPy-coated samples of 10 mg were hydrolyzed for 30 days at +60°C in 1.0 mL pure water. The hydrolyzed samples were analyzed with a single quadruple Perkin Elmer SQ 300 electrospray mass spectrometry (MS) system (PerkinElmer) in the positive ion mode. The drying gas (nitrogen) temperature was set at +175°C and the drying gas flow rate at 8 L/min. The capillary exit voltage was varied between 60 and 200 V to screen the onset of cracking of the PLA oligomers. The MS was operated in a scan mode (mass range 200–1000) and dwell time was set at 0.1 ms. Briefly, the (hydrolysis) solution was filtered through 0.45-μm PTFE filter, 0.5 mL methanol was added to the mixture (water/MeOH 2:1 v/v) and the sample injected by a syringe pump into the mass spectrometer at a flow rate of 5 μL/min.

Scanning electron microscopy. Noncoated PLA and PPy-coated PLA scaffolds were imaged by JSM–6360 LV SEM (JEOL). Low 3 kV acceleration voltage was applied to prevent sample damage and to induce contrast between electrically conductive and insulating areas. For the non-coated scaffold, the imaging was first done without metallic surface coating and, subsequently, a thin 20-nm sputter-coated gold layer (SCD 050; Balzers AG).

Atomic force microscopy. The morphology of individual PLA-PPy fibers in air was imaged by noncontact mode atomic force microscopy (Park XE-100 AFM; Park Systems). Silicon probes (ACTA-905M, Applied NanoStructures, Inc.) with a nominal resonance frequency of 300 kHz and spring constant of 4 N/m were applied with a pyramidal shaped tip (radius < 10 nm) and an aluminum reflective coating. 5×5 μm^2 scans were taken with a scan rate of 0.5 Hz. The surface roughness of the hydrolyzed sample was determined from the data by Park Systems XEI image processing software (Park Systems). For the roughness data, the analyzed area size was varied to test the consistency of

the result. Roughness analysis was done on the raw data. For the presentation of the surface topography of the curved surfaces, the raw data was 0th order flattened along the fiber axes, which were parallel to the slow axis of the AFM.

Electrical stimulation

Stimulation setup. The scaffolds were placed in custom-made bottomless 24-well plates (Greiner Bio-One GmbH). The two electrodes were in galvanic contact with the cell culture medium in each well (Fig. 1A). The top and the bottom electrodes were sputter-coated polyethylene-naphthalate (PEN)/Au films (125 μm DupontTeonex®, with 50 nm Au-coating applied by VTT). The bottom electrode (PEN/Au film) was attached to the well plate with biomedical grade Silastic® Q7-4720 liquid silicone rubber. The top electrodes were bent strips of PEN/Au-film, partly extending to the cell culture medium (Fig. 1A). The four strips were connected in parallel (Fig. 1B). Hence, the individual wells were also electronically connected in parallel. The electrode surface area was approximately 1 cm^2 for the top electrode and approximately 1.5 cm^2 for the bottom electrode in each well. The distance between the top and the bottom electrodes was approximately 2 mm, matching the thickness of the scaffolds under mild (< 10 kPa) compression. Hence, the fibers of the scaffolds were in physical contact with both the top and bottom electrodes.

Human ASCs were exposed to symmetric biphasic pulsed DC voltage repeated at a frequency of 1 or 100 Hz, ES for 4 h/day. Stimulation waveforms were generated by AFG 3010B (Tektronix Inc.) and the stimulation signal supplied by a laboratory voltage amplifier (VTT). The waveforms for the 1 and 100 Hz stimulation were pulsed DC voltages 250 ms (+200 mV)/250 ms (−200 mV)/500 ms (0 mV) and 2.5 ms (+200 mV)/2.5 ms (−200 mV)/5 ms (0 mV), respectively. A schematic illustration of the voltage is presented in Figure 1C. According to cyclic voltammetry (CV), the PEN/Au-electrodes were electrochemically stable in the ±200 mV potential window (CV data not shown). The transient current generated by the pulsed DC signal was monitored for the 24-well plate assembly with Tektronix TDS 3054B oscilloscope and 100 Ω series resistor. The measured peak current into the 24-well plate assembly in series with the 100 Ω was 2 mA. The measured steady state (DC) current after the 2.5 ms and the 250 ms pulses was in the range of 40–50 μA/cm^2, corresponding to cell impedance of 5 kΩ. Such a low current level could be only roughly measured with the 100 Ω resistor and the oscilloscope. Therefore, the range of the current densities was also based on the impedance spectroscopic data recorded earlier in the DMEM.

The electrical charge of one pulse containing both the transient electrical double layer charging of the Au-electrodes (Q1, Q2 in Fig.1C) and the contribution of the ionic DC current (dashed line in Fig.1C) of the 1 and 100 Hz waveforms were estimated 28.0 and 8.2 μC, respectively. The charging conditions for the top and the bottom electrodes were not balanced electronically and the open circuit voltage of the system was not measured. A nonstimulated group was used as a control.

Impedance of the electrode, cell culture medium, and the nonwoven scaffolds. Impedance spectra of circular parallel 1 cm^2 PEN/Au-film electrodes and parallel rigid TiN-coated steel electrodes (electrode material TiN) in the DMEM were measured using an HP 4192A impedance analyzer. In the measurement a 100 Ω series resistor and excitation voltage of sinusoidal 50 mV_{p-p} was used.

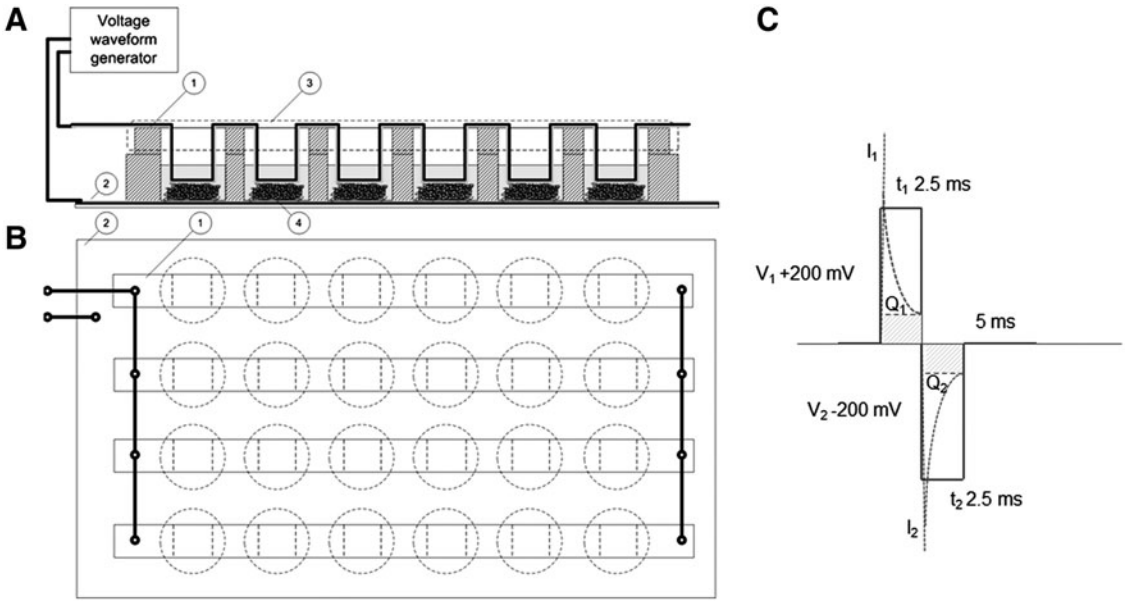

FIG. 1. **(A)** Schematic illustration of the stimulation device geometry as the side projection. Top and bottom electrodes were made of gold-coated polyethylene-naphthalate film. **(B)** The voltage waveform applied to the samples. Biphasic pulses are shown in blue color. The dashed line presents an estimation of the transient net current. Q_1 and Q_2 present both the transient electrical double layer charging of the Au-electrodes. **(C)** Schematic illustration of the stimulation device geometry as the above projection.

Subsequently, the impedance of the insulating PLA scaffold and the electrically conductive PLA-PPy scaffold was measured between the rigid TiN electrodes (OerlikonBalzersSandvik Coating). TiN electrodes were utilized as they provided an electrochemically stable, smooth, and mechanically rigid construction for the measurement cell. Constant phase element analysis (CPE) was done using the curve fitting tool provided in OriginPro 8.5.1 software (Originlab Corporation) using protocols described by Tandon et al.[26]

hASC culture

The experiments were repeated three times, each with a different human hASC line. The cells were isolated from the adipose tissue collected in surgical procedures from three females (aged 39, 43, and 79) at the Department of Plastic Surgery, Tampere University Hospital. Human ASC isolation from the tissue samples was conducted in accordance with the Ethics Committee of Pirkanmaa Hospital District, Tampere, Finland. The minced tissue samples were digested with collagenase type I (1.5 mg/mL; Invitrogen) and cell isolation was performed as previously described.[27] After primary culture in T-75 flasks, hASCs of passage 1 were harvested and analyzed by flow cytometry (FACSAria; BD Biosciences). Monoclonal antibodies against CD14-PE-Cy7, CD19-PE-Cy7, CD45RO-APC, CD49D-PE, CD73-PE, CD90-APC, CD106-PE-Cy5 (BD Biosciences Pharmingen); CD34-APC, HLA-ABC-PE, HLA-DR-PE (Immunotools GmbH Friesoythe); and CD105-PE (R&D Systems, Inc.) were used. Analysis was performed on 10,000 cells per sample, and the positive expression was defined as a level of fluorescence 99% greater than the corresponding unstained cell sample.

Cell expansion and experiments were carried out in the maintenance medium. When the ASCs reached 80% confluence, the cells were passaged. Cells of passages 4 to 5 were used for all experiments. Each scaffold was pretreated with the maintenance medium for 48 h at 37°C in custom-made 24-well plates. The scaffolds were seeded with 87,500 cells in a volume of 30 μL of the maintenance medium and the cells were allowed to attach for 3 h.

Viability. Cell attachment and viability were evaluated qualitatively using live/dead viability assay (Molecular Probes) at 7- and 14-day time points. CellTracker™ Green [5-chloromethylfluorescein diacetate (CMFDA; Molecular Probes) and ethidium homodimer-1 (EthD-1; Molecular Probes) were utilized to dye viable cells (green fluorescence) and dead cells (red fluorescence), respectively, as previously described.[7]

Proliferation and differentiation. The DNA content in the hASC-seeded scaffold constructs was measured after 1, 7, and 14 days' culture using the CyQUANT® Cell proliferation assay kit (Molecular Probes–Invitrogen) according to the manufacturer's protocol and as earlier described.[27] To uniformly extract the DNA, cells were lysed in the scaffold using 0.1% Triton X-100 followed by a freeze–thaw cycle, and then the scaffold was disrupted and the cell lysate carefully collected from the scaffolds for the analysis. The fluorescence was measured with Victor 1420 Multilabel Counter; Wallac). The quantitative alkaline phosphatase (ALP) measurement was performed at time points of 7 and 14 days according to the Sigma ALP procedure (Sigma Aldrich)[27] with minor modifications. Quantitative ALP activity results were normalized to the total amount of DNA measured from the same samples.

Statistical analysis. The statistical analyses were performed with SPSS, version 17. All assays were performed in triplicate and the data were presented as mean ± standard deviation (SD) for both quantitative analyses. The equal variance assumption was checked by the Levene's Test. All statistical analyses were performed at a significance level $p < 0.05$ using one-way analysis of variance (ANOVA) or the T-test. Bonferroni *post hoc* correction for multiple corrections was used. The effects of different culturing periods (1 day vs. 7 days vs. 14 days), scaffold materials (PLA vs. PLA-PPy), and stimulation setup (ES 1 Hz vs. ES 100 Hz vs. control) were evaluated from the combined data of the three experiments.

Results

Effect of hydrolysis on DC electrical conductivity

Incubation of the PPy-coated PLA fiber scaffolds in PBS (pH 7.4) resulted in a significant decrease in DC conductivity during the first day (Fig. 2). Directly after the synthesis the in-plane resistance of the air-dried samples was 50 ± 20 kΩ. Rinsing with deionized water increased the resistance to 90 ± 40 kΩ on day 0. At day 1, the measured resistance was 2.5 ± 0.8 MΩ and steadily increased to 29 ± 14 MΩ on day 7. According to optical microscopy, the surface of the fiber was still fully covered with the PPy coating on day 20. The DC conductivity of the hydrolyzed scaffolds could be partly restored by rinsing with a diluted hydrochloric acid (pH 2) solution and subsequent air drying. Roughly, 5%–10% of the conductivity of the hydrolyzed scaffold was restored by the acid rinse irrespective of the hydrolysis time.

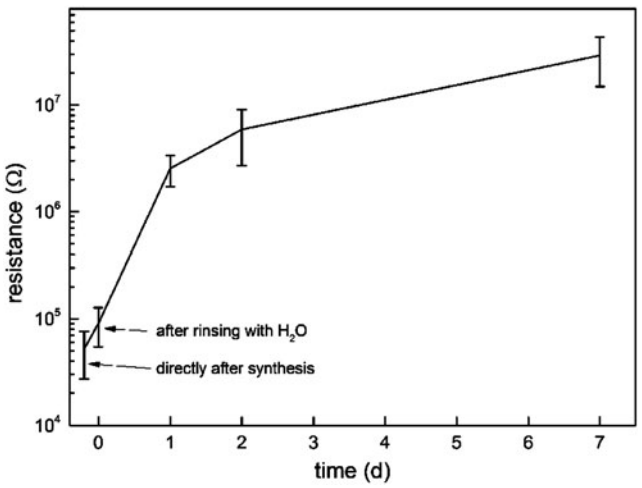

FIG. 2. Resistance of the poly-96L/4D-lactide-polypyrrole (PLA-PPy) scaffold in air ($n = 4$). The samples were rinsed with deionized and air-dried before each measurement. The conductivity of the sample remains at a level relevant for electrical stimulation for at least 2 days.

Table 1. Summary of Impedance Spectroscopic Data Measured in Dulbecco's Modified Eagle's Medium and the Corresponding Constant Phase Element Analyses

Sample	$\|Z\|_{cell}$ *at 1 Hz (Ω)*	$\|Z\|_{cell}$ *at 10 kHz (Ω)*	*CPE capacitance (μF)*	*idealitycoeff. η*
PEN/Au/film	240000	15	2	0.97
TiN	83000	17	20	0.94
TiN/PLA scaffold	13000	26	20	0.90
TiN/PLA-PPy scaffold	1700	12	14	0.83

HP 4192A impedance analyzer, excitation voltage is sinusoidal 50 mVp-p
CPE, constant phase element; PEN, polyethylene-naphthalate; PLA-PPy, poly-96L/4D-lactide-polypyrrole.

Impedance of the electrode, cell culture medium, and the nonwoven scaffolds

The results of the impedance measurement are summarized in the following Table 1.$|Z|_{cell}$ is the magnitude of cell impedance, CPE represents the capacitance of the cell, and η is a fit parameter describing the ideality of capacitance in the CPE model.[26]

According to the measured data, the PLA and the PLA-PPy scaffolds both had a significant effect on cell impedance in the DMEM. The low-frequency impedances specially were significantly lower for the cell containing the scaffolds in the DMEM (either PLA or PLA-PPy) than for the empty cell containing only the medium. As anticipated, the PLA-PPy scaffold induced the most significant decrease in cell impedance at lower frequencies. The ideality coefficient η was low (0.83) for the PLA-PPy scaffold, suggesting that the capacitive CPE model did not describe the cell impedance spectrum in this case. Contrary to expectations, the PLA scaffold also decreased the cell impedance. This was surprising since the relative permittivity of the medium (around 80) is much higher compared with the dry PLA polymer (around 3.5). The result can be explained by a marked enhancement of (low-frequency) ionic conductivity along the PLA fibers. The low-frequency impedance was three-fold higher, and the capacitance was 10-fold lower for the Au-electrodes than for the TiN electrodes.

We used impedances derived from sinusoidal test signals (2.4.2) for estimating the order of magnitude for the stimulation current during the biphasic pulses. The Ohm's law and the impedances measured at 1 Hz and 10 kHz were used for estimating the current densities in the Au-electroded stimulation 24-well setup. Theoretical current densities $I_{1,2,DC} \pm 13.3\,\mu A/cm^2$ $I_{1,2,max} \pm 16.7\,mA/cm^2$ for the DC current and the transient current were calculated, respectively. The real transient current density, which is not directly measurable using our system, was limited by the current amplifier to roughly $\pm 0.4\,mA/cm^2$. The discrepancy between the observed and the calculated values was likely due to the discrepancies between the impedance measurement and the ES setup. However, both the measured and the estimated DC and transient currents were within a physiologically relevant range, but could be considered minimally invasive for the hASCs.[28]

Electrospray ionization mass spectroscopy

The electrospray ionization-MS (ESI-MS) spectra for the PLA-PPy and PLA scaffolds were very similar (Fig. 3). The spectra contained peaks of PLA hydrolysis products[29] and the corresponding Na peaks. No significant peaks associated with potential PPy or CS degradation products, such as oxidized pyrrole oligomers or oligosaccharides, were found in the studied m/z range of 200–1000.

Scanning electron microscopy

According to scanning electron microscopy (SEM) images, the surfaces of the PPy-coated PLA fibers were covered with a conductive layer. This was clearly detected (Fig. 4, left), since the fiber scaffold did not build up any electrostatic charge under the electron beam at 3-kV acceleration voltage. The surface of the metallized (20 nm Au) PLA fibers appeared smooth in comparison to the PPy-coated fibers (Fig. 4, right).

Atomic force microscopy

Figure 5 shows representative topography and the measured surface roughness of individual PPy-PLA fibers after hydrolysis in PBS. The long axis of the fiber in each AFM was set parallel to the slow scan axis (45 degrees in the images in Fig. 5A). On day 0, the fiber surface appears extensively covered by fine nodular material individual nodules being 200 nm in diameter. This presented the typical morphology for PPys prepared by chemical polymerization. On day 10, the nodular surface morphology of the fibers was detected as on day 1. However, smoother areas and coarser (>400 nm) nodules with fine structure had appeared on day 10. On day

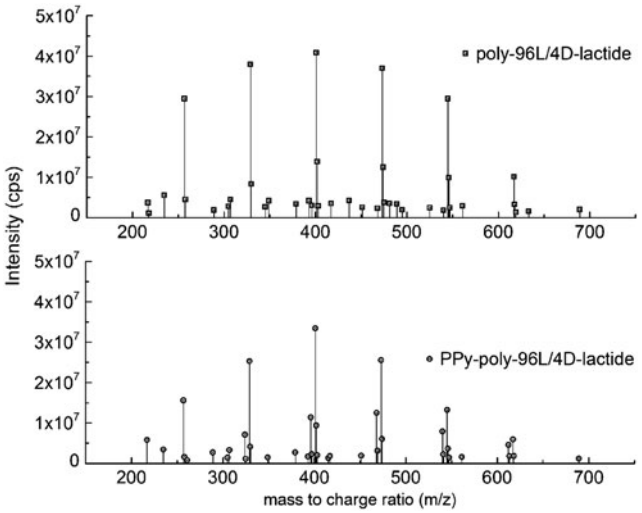

FIG. 3. Electrospray ionization-mass spectrometry spectra of the hydrolysis products from PLA-PPy and PLA scaffolds. All detectable peaks are found in the m/z range of 200–700.

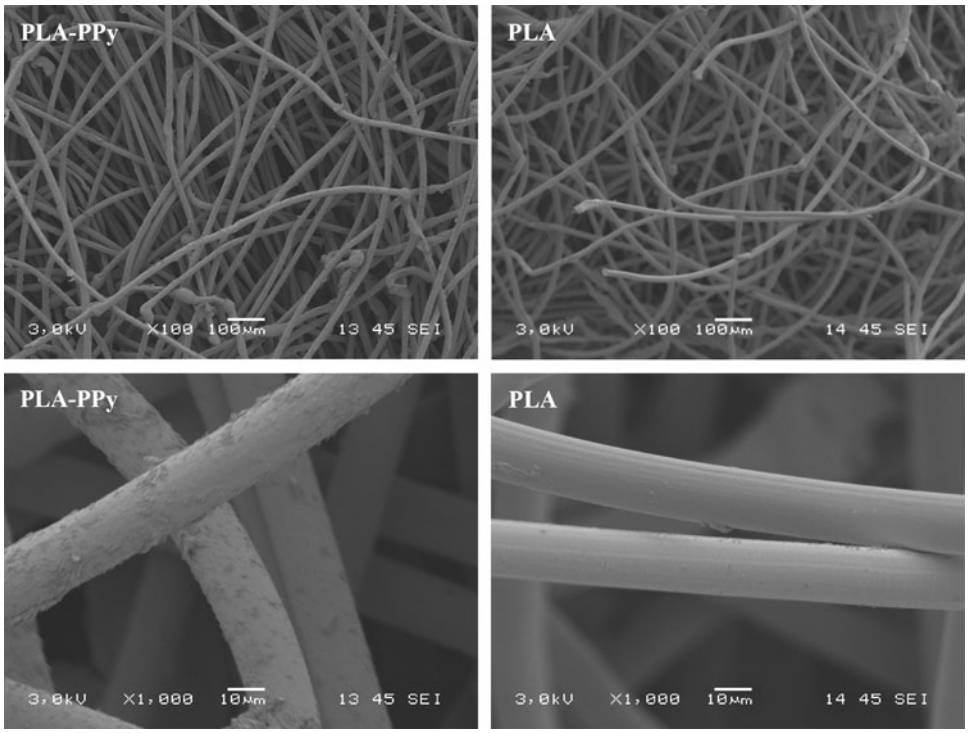

FIG. 4. Scanning electron microscopy image of PLA-PPy scaffold (left) without sputtered gold layer and PLA scaffold (right) with 20 nm gold coating. At 3-kV acceleration voltage, the PPy-coated PLA scaffold could be readily imaged, but the electrically insulating PLA scaffold could not be imaged without a thin coating layer (typically gold or carbon) due to heavy electrostatic charging.

20, the fraction of smoother areas had further increased from day 10. According to optical microscopy, the fibers were still fully covered with PPy after the 20 days in PBS. Hence, the observed changes were probably due to the changes of the PPy coating morphology and/or the hydrolysis of the PLA surface under the PPy coating.

The changes in the AFM images were reflected in the surface roughness values (Ra) derived from the images (Fig. 5B). Within 10 days, the Ra values decreased significantly from about 160 nm to less than 80 nm. The roughness analysis showed a consistency independent of how the analyzed surface area was chosen from the images ($5\times5\,\mu m^2$, $2\times2\,\mu m^2$ subareas).

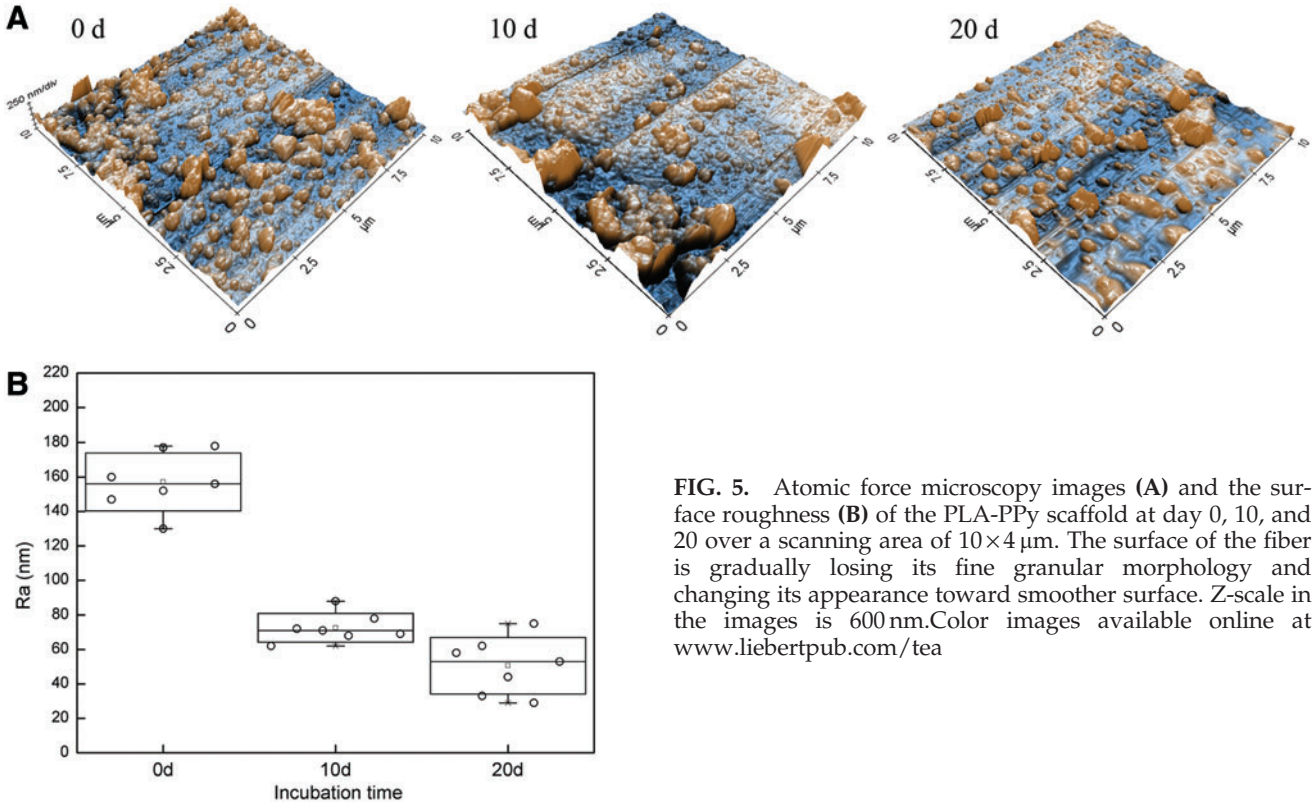

FIG. 5. Atomic force microscopy images **(A)** and the surface roughness **(B)** of the PLA-PPy scaffold at day 0, 10, and 20 over a scanning area of $10\times4\,\mu m$. The surface of the fiber is gradually losing its fine granular morphology and changing its appearance toward smoother surface. Z-scale in the images is 600 nm.Color images available online at www.liebertpub.com/tea

Cell culture

Flow cytometry. The flow cytometric analysis demonstrated that hASCs show high expression of CD105 (endoglin), CD73 (ecto 5′ nucleotidase), and CD90 (Thy-1), moderate expression (<50% >2%) of CD34 (hematopoietic progenitor and endothelial cell marker), and CD49d (integrin α4), while lacking expression (≤2%) of CD14 (monocyte and macrophage marker), CD19 (B cell marker), CD45RO (pan-leukocyte marker), CD106 (vascular cell adhesion molecule 1), and HLA-DR (HLA class II). Surface marker expression characteristics of undifferentiated ASCs from one donor cell line is presented in Figure 6. The results showed that hASCs expressed several of the specific antigens proposed by the Mesenchymal and Tissue Stem Cell Committee of the ISCT[30] defining human stem cells of mesenchymal origin. According to ISCT, CD34 should not be expressed in stem cells of mesenchymal origin; however, it showed moderate expression with high donor variation. However, varying results have been reported for CD34 on hASCs cultured in a medium supplemented with human serum[31–33] and fetal bovine serum.[31,34,35]

Viability. Live/dead staining showed that the majority of hASCs were viable and spread homogenously in both scaffold types with and without ES on day 14 (Fig. 7). By qualitative estimation, the number of hASCs was higher in PLA-PPy scaffolds than in the plain PLA scaffolds at all time points. This difference was evident on the cell seeding surface (Fig. 7) and the bottom surface of the scaffolds as well as inside the scaffolds (Supplementary Figs. S1 and S2; Supplementary Data are available online at www.liebertpub.com/tea). The ES did not seem to have any effect on cell viability or the cell number.

Proliferation and early osteogenic differentiation. The number of hASCs was assessed quantitatively using the CyQUANT proliferation method (Fig. 8), which is based on the relative absorbance values according to the amount of DNA. As demonstrated with live/dead staining, the number of hASCs was higher in PLA-PPy scaffolds at each time point compared to PLA scaffolds. This difference was statistically significant, excluding 7-day time point, in the nonstimulated and in the stimulated (100 Hz) group. In addition, the cell number in PLA scaffolds did not increase over time, whereas the cell proliferation during the 14-day culture period was detected in PLA-PPy scaffolds. Neither did the stimulation of 1 Hz nor 100 Hz show any effect on cell proliferation.

ALP analysis was performed on the same samples as used for DNA amount analysis (Fig. 9). ALP activity of hASCs was higher in PLA-PPy scaffolds in each stimulation group than in the PLA scaffolds at 7 and 14 days. One donor line did not show reliably detectable ALP activity at any of the measured time points. Therefore, data from two other repeats only are shown. The ALP activity values varied notably between the two donor lines; hence, no significant differences were detected between different scaffold types or stimulation groups.

Discussion

As our main finding, the PPy coating enhanced hASC proliferation. A similar trend was also seen in ALP activity, but no significant differences were detected. ALP activity peaked at the 7-day time point, which is typical behavior for ASCs in 3D scaffolds in the maintenance medium.[36] To the best of our knowledge, this is the first study to investigate the effect of ES on hASCs in a 3D culture system on PLA-PPy scaffolds by exploiting the conductivity properties of PPy. For the ES in the 3D culture system, we designed a custom-made stimulation setup, where multiple scaffolds could simultaneously be stimulated. Symmetric biphasic pulsed DC voltage with ±100 mV/mm pulse amplitude (2.5 ms/250 ms pulse duration and

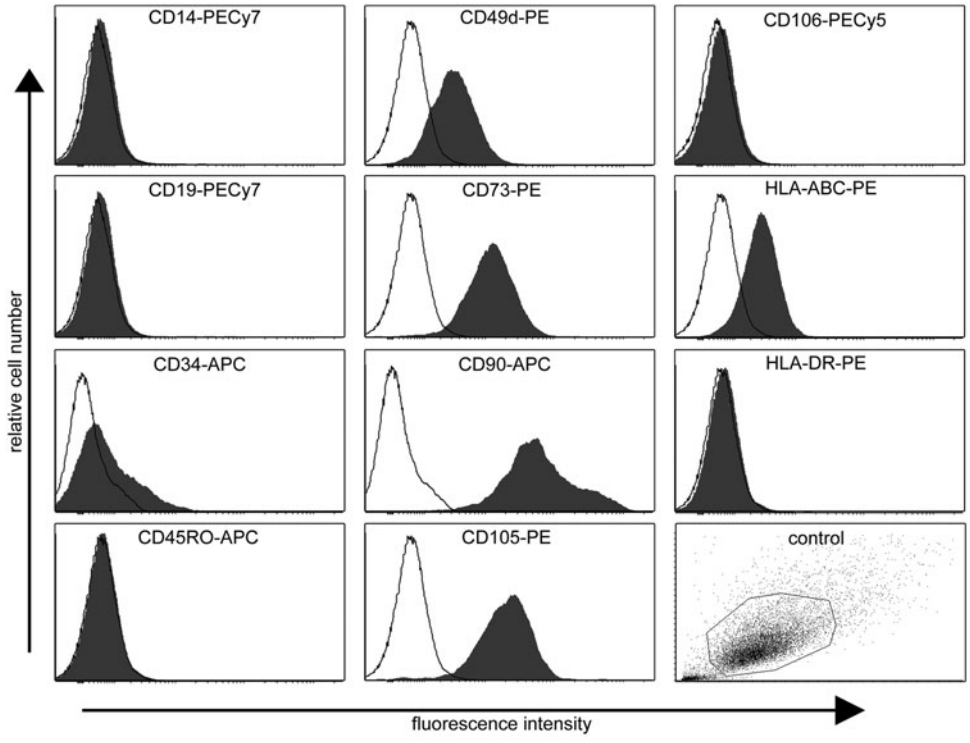

FIG. 6. Surface marker expression characteristics of undifferentiated adipose stem cells (ASCs) from one donor cell line as analyzed by flow cytometry. Relative cell number (*y*-axis) and fluorescence intensity (*x*-axis). Unstained control cells (empty histograms) and cells stained with antibody (filled histograms). Unstained control sample dot plot showing particle size and granularity (side scatter vs. forward scatter).

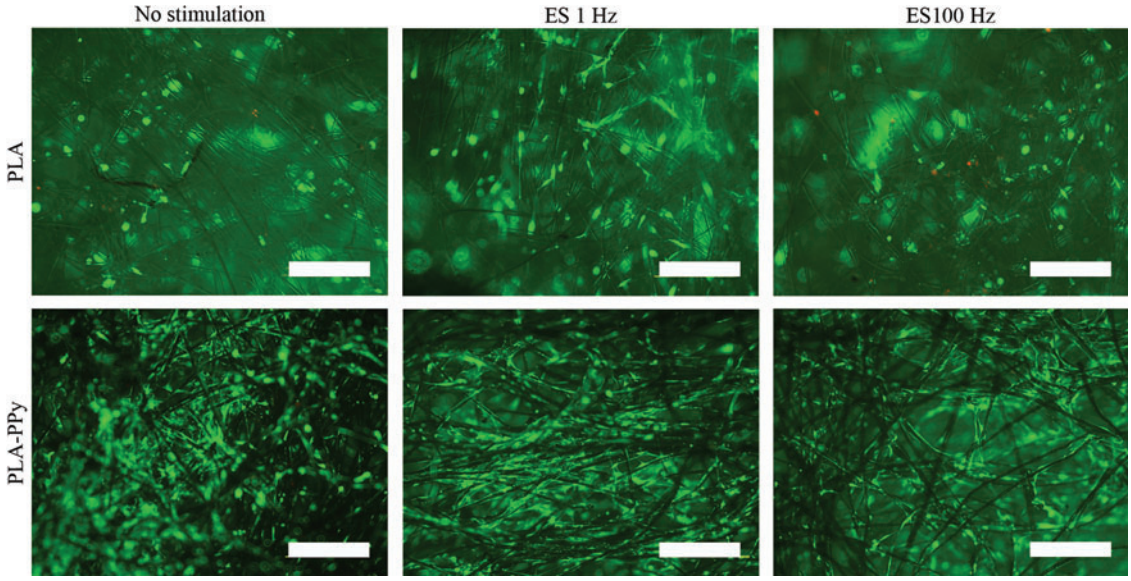

FIG. 7. Representative images of viable (green fluorescence) and dead (red fluorescence) human adipose stem cells at 14-day time point attached to PLA and PLA-PPy scaffolds visualized at top/cell seeding side of the scaffolds. Scale bar is 500 μm. Color images available online at www.liebertpub.com/tea

100 Hz/1 Hz pulse frequencies, respectively), was chosen on the basis of earlier studies demonstrating their physiological relevance, safety, and applicability to stimulating hASCs.[19,21]

ES can be considered a potential way to stimulate hASCs as it offers a means to exert similar influence on cells as, for example, growth factors, but in a safer, more inexpensive and repeatable way.[19] Nevertheless, no significant differences in early osteogenic differentiation or proliferation were detected between electrically stimulated and nonstimulated hASCs in our setup. This result was in contrast to many recent studies reporting favorable effects of ES on hASC osteogenic differentiation. McCullen et al. demonstrated hASC mineralization and differentiation toward bone tissue under ES in a 2D culture system[19] when the osteogenic medium was used (the maintenance medium supplemented with 50 mM ascorbic acid, 0.1 mM dexamethasone, and 10 mM β-glycerofosfate, while Tandon *et al.*[21] demonstrated that hASCs align and elongate in the presence of ES. Similar to our study, no differentiation medium or growth factors were used to increase the differentiation processes. As a result, they did not detect osteogenic differentiation, but rather fibroblastic or vasculogenic differentiation. As our study set out to investigate early osteogenic differentiation, it remains to be determined if differentiation into other lineages occurred.

Hammerick *et al.* used mouse ASCs and stimulated them using very similar parameters to ours. Their results on proliferation were consistent with ours since they did not detect any effect of ES on proliferation during a 10-day culture period. On the other hand, osteogenic differentiation was observed only in combination with ES and the osteogenic medium (the maintenance medium supplemented with 100 mg/mL of ascorbic acid and 10 mM β-glycerophosphate).

It should also be noted that most of the studies of using ES for stem cells have not been done in combination with electrically conductive biomaterial. PPy and ES may have synergistic effects, such as redox activity upon potential changes and bioactive molecules as dopants, which can affect also to the cell response in addition to the applied ES.[6]

The electrical impedance of the Au-electrodes in the DMEM changed significantly in the frequency range of sinusoidal (50 mV) 1–1000-Hz test signals, as confirmed by impedance spectroscopy. Indeed, the nonlinearity of the

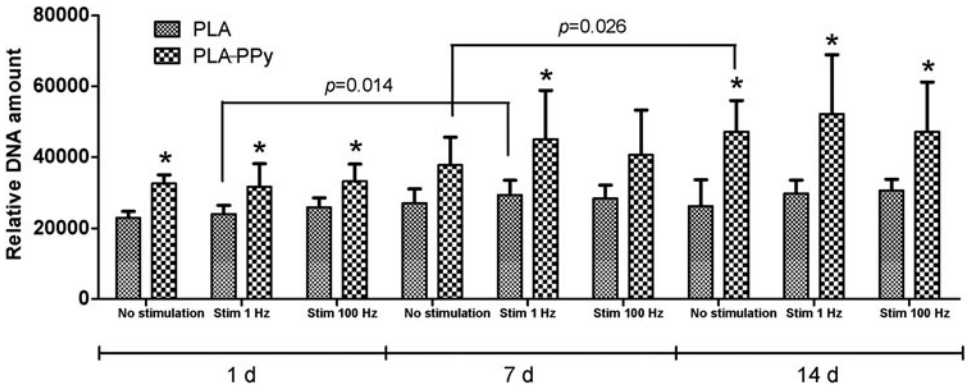

FIG. 8. Relative DNA content of human adipose stem cells cultured for 1, 7, and 14 days in PLA and PLA-PPy scaffolds. The results are expressed as mean ± SD, $n = 3$. The total number of technical samples was 9. *$p < 0.05$ with respect to the corresponding PLA scaffold.

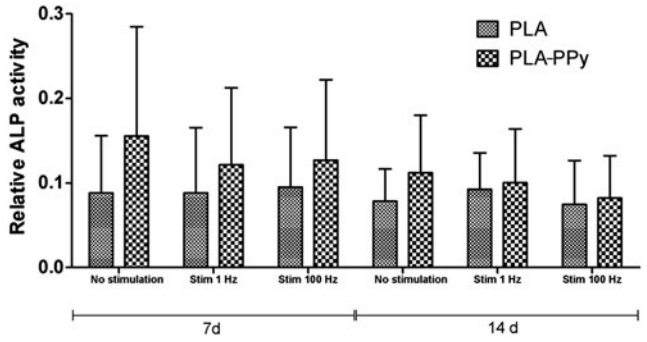

FIG. 9. Relative ALP activity of human adipose stem cells cultured for 7 and 14 days in PLA and PLA-PPy scaffolds. The results are expressed as mean ± SD, $n = 2$. The total number of technical samples was 6.

stimulation cell impedance was found to be an important factor in designing electronic stimulation setups and waveforms for stem cells. As anticipated, the electrically conductive PPy-PLA scaffold placed between the circular 1 cm^2 TiN electrodes decreased the impedance of the TiN/DMEM/TiN cell significantly, in particular, in the lower frequency range. A less significant, but a surprising decrease in cell impedance was also observed for the PLA scaffold, which is an excellent electrical insulator in air. In both cases, a possible explanation would be a marked enhancement of the conductivity of the fibers, extending to the interior of the scaffold. In the case of PLA fibers, the enhancement was likely due to increased surface ionic conductivity. For the PLA-PPy fiber, the enhancement was more easily understood since PPy is an electronic conductor both in air and in a medium. Our results suggest that an electronically conductive PPy can better deliver the stimulation currents to the cells located in the interior of the scaffold, which may have an additional effect on cell response. It is noteworthy that a significant enhancement of the electronic conductivity resulted from only 2–3 wt-% of the conductive PPy in the composite PLA-PPy fibers.

The in-plane DC resistance of air-dried PLA-PPy scaffolds was 50 kΩ on day 0. The DC conductivity of the PPy coating was roughly 10–30 S/m, based on an order of magnitude estimation of the DC conductivity of the PPy-layer and a careful extrapolation of the impedance spectroscopic data to very low frequencies. The estimated conductivity was within the range of the electronic volume conductivity reported for bulk PPy-sulfate powders prepared by APS oxidation in water.[37] Hence, the incorporation of the CS dopant did not adversely affect the electronic conductivity of PPy. The loss of DC conductivity of PPy coating was partly restored by acid doping in pH 2. Therefore, the loss of electronic conductivity was partly due to reversible de-doping of PPy chains in high pH 7.4.[6] Other mechanisms, such as PLA degradation, were also affecting the PPy coating and/or detachment, and cracking of the PPy layer. According to the impedance spectroscopy (1–10 kHz) and the DC measurements, the AC conductivity (electronic and ionic) of the PPy layer remained considerably (>2 decades) higher than the ionic conductivity of the DMEM at least on days 0–2. Although the impedance measurement cannot discriminate between the electronic conductivity and the ionic conductivity of the scaffold material, we find this a clear indication that the scaffold will enhance the stimulation current flow for periods far exceeding 2 days.

Irreversible changes were also apparent in the morphology of the fibers according to AFM topography images, which showed that the appearance of the fibers changed significantly during incubation. According to optical microscopy, the fibers were still fully covered with PPy after the 20 days in PBS. The data suggested extensive morphological changes in the thin PPy layer due to dopant ion exchange, hydration, osmotic pressure, and/or hydrolysis of the PLA surface under the PPy coating. Both factors may have affected the morphology of PPy, the local adhesion of the PPy coating, and consequently, the electronic conductivity of the coating.

Between the electrochemical potentials of the ES signals (±200 mV) used, the PPy remained in oxidized state. Thus, it is unlikely that redox chemistry had any significant effects on PPy morphology. Hydration and hydrolytic degradation of the outermost surface of the PLA may have been affected by the PPy coating and the ES, mainly due to the high ionicity of PPy. However, we found no direct evidence of such effect using SEM, AFM, and ESI-MS. This should be further studied in future.

Under the oxidative polymerization conditions, the CS was rapidly split into fragments (C4–C6) as evidenced by the viscosity measurements (data not shown). Although it was evident that the CS induced permanent hydrophilicity of the PPy coating, the role of the CS dopant in the cell response of PPy coating remained unclear. After hydrolysis in deionized water at +60°C, we did not detect pyrrole oligomers or CS fragments in the hydrolysis products of the PLA-PPy fibers by ESI-MS. It is therefore debatable if molecular fragments of the CS remained in PPy. This needs elucidation since CS fragments have well reported biological activity both *in vitro* and *in vivo*.[38,39] Nevertheless, our results showed that the effect of PPy coating on hASC response was as strong with and without ES, suggesting that the surface chemistry of PPy plays a more important role in triggering cell response than in the electrical conductivity of PPy.

According to the ESI-MS spectra, the influence of PPy coating on the hydrolysis of the PLA scaffold was negligible. According to our interpretation, the thin PPy coating was not hydrolytically degraded in water and had little effect on the hydrolytic degradation of the PLA scaffolds *in vitro*.

In conclusion, the novel PPy-coated scaffolds significantly enhanced hASC proliferation. In addition, early osteogenic differentiation was consistently more enhanced by PPy coating than by plain PLA scaffolds. This study highlights the future potential of PPy-coated PLA scaffolds seeded with hASCs in clinical bone tissue engineering applications. The ES of the relatively noninvasive biphasic pulsed voltage waveforms in 3D geometry did not have a significant effect on hASC proliferation or differentiation on days 1, 7, and 14.

Acknowledgments

The authors would like to thank Ms. Anne Rajala M.Sc, Ms. Ana Luísa Delgado Lima, and Ms. Hanna Juhola for the preparation and hydrolytic testing of the scaffolds, Ms. Anna-Maija Honkala and Ms. Minna Salomäki M.Sc for their assistance in the cell culture work. This study was financially supported by the Finnish Funding Agency for Technology

and Innovation (TEKES), the Academy of Finland and the Competitive Research Funding of Tampere University Hospital (grant 9K020).

Disclosure Statement

No competing financial interests exist.

References

1. Gloria, A., De Santis, R., and Ambrosio, L. Polymer-based composite scaffolds for tissue engineering. J Appl Biomater Biomech **8,** 57, 2010.
2. Niemelä, T., Niiranen, H., Kellomäki, M., and Törmälä, P. Self-reinforced composites of bioabsorbable polymer and bioactive glass with different bioactive glass contents. Part I: initial mechanical properties and bioactivity. Acta Biomater **1,** 235, 2005.
3. Cronin, E.M., Thurmond, F.A., Bassel-Duby, R., Williams, R.S., Wright, W.E., Nelson, K.D., and Garner, H.R. Protein-coated poly(L-lactic acid) fibers provide a substrate for differentiation of human skeletal muscle cells. J Biomed Mater Res Part A **69A,** 373, 2004.
4. Jiang, T., Khan, Y., Nair, L.S., Abdel-Fattah, W.I., and Laurencin, C.T. Functionalization of chitosan/poly(lactic acid-glycolic acid) sintered microsphere scaffolds via surface heparinization for bone tissue engineering. J Biomed Mater Res Part A **93A,** 1193, 2010.
5. Jakubiec, B., Marois, Y., Zhang, Z., Roy, R., Sigot-Luizard, M., Dugré, F.J., King, M.W., Dao, L., Laroche, G., and Guidoin, R. *In vitro* cellular response to polypyrrole-coated woven polyester fabrics: Potential benefits of electrical conductivity. J Biomed Mater Res **41,** 519, 1998.
6. Ateh, D.D., Navsaria, H.A., and Vadgama, P. Polypyrrole-based conducting polymers and interactions with biological tissues. J R Soc Interface **3,** 741, 2006.
7. Pelto, J., Haimi, S., Puukilainen, E., Whitten, P.G., Spinks, G.M., Bahrami-Samani, M., Ritala, M., and Vuorinen, T. Electroactivity and biocompatibility of polypyrrole-hyaluronic acid multi-walled carbon nanotube composite. J Biomed Mater Res Part A **93A,** 1056, 2010.
8. Du Souich, P., García, A.G., Vergés, J., and Montell, E. Immunomodulatory and anti-inflammatory effects of chondroitin sulphate. J Cell Mol Med **13,** 1451, 2009.
9. Schneiders, W., Reinstorf, A., Ruhnow, M., Rehberg, S., Heineck, J., Hinterseher, I., Biewener, A., Zwipp, H., and Rammelt, S. Effect of chondroitin sulphate on material properties and bone remodelling around hydroxyapatite/collagen composites. J Biomed Mater Res Part A **85A,** 638, 2008.
10. Manton, K.J., Haupt, L.M., Vengadasalam, K., Nurcombe, V., and Cool, S.M. Glycosaminoglycan and growth factor mediated murine calvarial cell proliferation. J Mol Histol **38,** 415, 2007.
11. Manton, K.J., Leong, D.F.M., Cool, S.M., and Nurcombe, V. Disruption of heparan and chondroitin sulfate signaling enhances mesenchymal stem cell-derived osteogenic differentiation via bone morphogenetic protein signaling pathways. Stem cells **25,** 2845, 2007.
12. Garner, B., Georgevich, A., Hodgson, A.J., Liu, L., and Wallace, G.G. Polypyrrole-heparin composites as stimulus-responsive substrates for endothelial cell growth. J Biomed Mater Res **44,** 121, 1999.
13. Gilmore, K.J., Kita, M., Han, Y., Gelmi, A., Higgins, M.J., Moulton, S.E., Clark, G.M., Kapsa, R., and Wallace, G.G. Skeletal muscle cell proliferation and differentiation on polypyrrole substrates doped with extracellular matrix components. Biomaterials **30,** 5292, 2009.
14. Richardson, R.T., Thompson, B., Moulton, S., Newbold, C., Lum, M.G., Cameron, A., Wallace, G., Kapsa, R., Clark, G., and O'Leary, S. The effect of polypyrrole with incorporated neurotrophin-3 on the promotion of neurite outgrowth from auditory neurons. Biomaterials **28,** 513, 2007.
15. Shi, G., Rouabhia, M., Meng, S., and Zhang, Z. Electrical stimulation enhances viability of human cutaneous fibroblasts on conductive biodegradable substrates. J Biomed Mater Res Part A **84A,** 1026, 2008.
16. Shi, G., Zhang, Z., and Rouabhia, M. The regulation of cell functions electrically using biodegradable polypyrrole–polylactide conductors. Biomaterials **29,** 3792, 2008.
17. Meng, S., Zhang, Z., and Rouabhia, M. Accelerated osteoblast mineralization on a conductive substrate by multiple electrical stimulation. J Bone Miner Metabol **29,** 535, 2011.
18. McCaig, C.D., Rajnicek, A.M., Song, B., and Zhao, M. Controlling cell behavior electrically: current views and future potential. Physiol Rev **85,** 943, 2005.
19. McCullen, S.D., McQuilling, J.P., Grossfeld, R.M., Lubischer, J.L., Clarke, L.I., and Loboa, E.G. Application of low-frequency alternating current electric fields via interdigitated electrodes: effects on cellular viability, cytoplasmic calcium, and osteogenic differentiation of human adipose-derived stem cells. Tissue Eng Part C Methods **16,** 1377, 2010.
20. Hammerick, K.E., James, A.W., Huang, Z., Prinz, F.B., and Longaker, M.T. Pulsed direct current electric fields enhance osteogenesis in adipose-derived stromal cells. Tissue Eng Part A **16,** 917, 2010.
21. Tandon, N., Goh, B., Marsano, A., Chao, P.H., Montouri-Sorrentino, C., Gimble, J., and Vunjak-Novakovic, G. Alignment and elongation of human adipose-derived stem cells in response to direct-current electrical stimulation. Annual International Conference of the IEEE Engineering in Medicine and Biology Society. Minneapolis, MN: IEEE Engineering in Medicine and Biology Society. 1, 6517, 2009.
22. Schmidt, C.E., Shastri, V.R., Vacanti, J.P., and Langer, R. Stimulation of neurite outgrowth using an electrically conducting polymer. Proc Natl Acad Sci U S A **94,** 8948, 1997.
23. Wong, J.Y., Langer, R., and Ingber, D.E. Electrically conducting polymers can noninvasively control the shape and growth of mammalian cells. Proc Natl Acad Sci U S A **91,** 3201, 1994.
24. Rowlands, A.S., and Cooper-White, J.J. Directing phenotype of vascular smooth muscle cells using electrically stimulated conducting polymer. Biomaterials **29,** 4510, 2008.
25. Wolszczak, M., Kroh, J., and Abdel-Hamid, M. Effects of the radiation processing of conductive polymers. Radiat Phys Chem **1,** 78, 1995.
26. Tandon, N., Cannizzaro, C., Chao, P.H., Maidhof, R., Marsano, A., Au, H.T., Radisic, M., and Vunjak-Novakovic, G. Electrical stimulation systems for cardiac tissue engineering. Nat Protoc **4,** 155, 2009.
27. Haimi, S., Moimas, L., Pirhonen, E., Lindroos, B., Huhtala, H., Räty, S., Kuokkanen, H., Sándor, G.K., Miettinen, S., and Suuronen, R. Calcium phosphate surface treatment of bioactive glass causes a delay in early osteogenic differentiation of adipose stem cells. J Biomed Mater Res Part A **91A,** 540, 2009.
28. Sun, S., Liu, Y., Lipsky, S., and Cho, M. Physical manipulation of calcium oscillations facilitates osteodiffer-

entiation of human mesenchymal stem cells. FASEB J **21,** 1472, 2007.
29. Andersson, S.R., Hakkarainen, M., Inkinen, S., Sodergard, A., and Albertsson, A.C. Polylactide stereocomplexation leads to higher hydrolytic stability but more acidic hydrolysis product pattern. Biomacromolecules **11,** 1067, 2010.
30. Dominici, M., Le Blanc, K., Mueller, I., Slaper-Cortenbach, I., Marini, F., Krause, D., Deans, R., Keating, A., Prockop, D., and Horwitz, E. Minimal criteria for defining multipotent mesenchymal stromal cells. The International Society for Cellular Therapy position statement. Cytotherapy **8,** 315, 2006.
31. Kocaoemer, A., Kern, S., Klüter, H., and Bieback, K. Human AB serum and thrombin-activated platelet-rich plasma are suitable alternatives to fetal calf serum for the expansion of mesenchymal stem cells from adipose tissue. Stem Cells **25,** 1270, 2007.
32. Lindroos, B., Boucher, S., Chase, L., Kuokkanen, H., Huhtala, H., Haataja, R., Vemuri, M., Suuronen, R., and Miettinen, S. Serum-free, xeno-free culture media maintain the proliferation rate and multipotentiality of adipose stem cells *in vitro*. Cytotherapy **11,** 958, 2009.
33. Parker, A.M., Shang, H., Khurgel, M., and Katz, A.J. Low serum and serum-free culture of multipotential human adipose stem cells. Cytotherapy **9,** 637, 2007.
34. Gronthos, S., Franklin, D.M., Leddy, H.A., Robey, P.G., Storms, R.W., and Gimble, J.M. Surface protein characterization of human adipose tissue-derived stromal cells. J Cell Physiol **189,** 54, 2001.
35. Mitchell, J.B., McIntosh, K., Zvonic, S., Garrett, S., Floyd, Z.E., Kloster, A., Di Halvorsen, Y., Storms, R.W., Goh, B., Kilroy, G., Wu, X., and Gimble, J.M. Immunophenotype of human adipose-derived cells: temporal changes in stromal-associated and stem cell-associated markers. Stem cells **24,** 376, 2006.
36. Marino, G., Rosso, F., Cafiero, G., Tortora, C., Moraci, M., Barbarisi, M., and Barbarisi, A. Beta-tricalcium phosphate 3D scaffold promote alone osteogenic differentiation of human adipose stem cells: *in vitro* study. J Mater Sci **21,** 353, 2010.
37. Blinova, N.V., Stejskal, J., Trchová, M., Prokeš, J., and Omastová, M. Polyaniline and polypyrrole: A comparative study of the preparation. Eur Poly J **43,** 2331, 2007.
38. Kang, S.K., Putnam, L., Dufour, J., Ylostalo, J., Jung, J.S., and Bunnell, B.A. Expression of telomerase extends the lifespan and enhances osteogenic differentiation of adipose tissue-derived stromal cells. Stem Cells **22,** 1356, 2004.
39. Grzesik, W.J., Frazier, C.R., Shapiro, J.R., Sponseller, P.D., Robey, P.G., and Fedarko, N.S. Age-related changes in human bone proteoglycan structure. Impact of osteogenesis imperfecta. J Biol Chem **277,** 43638, 2002.

Address correspondence to:
Suvi Haimi, PhD
Department of Biomaterials Science and Technology
University of Twente
P.O. Box 217
Enschede 7500 AE
The Netherlands

E-mail: suvi.haimi@uta.fi

Received: February 22, 2012
Accepted: October 17, 2012
Online Publication Date: January 4, 2013